P5.12 CLOUD−RESOLVING NUMERICAL EXPERIMENTS OF DEEP ATMOSPHERIC CONVECTION OVER TROPICAL OCEANS

Alexandre Araújo Costa*
Universidade Estadual do Ceará, Fortaleza, Brazil

1. INTRODUCTION

Atmospheric motions involve multiple scales, from the large−scale circulations that establish the environment in which convection develops, down to turbulence, with cloud−scale and mesoscale circulations in between. Since atmospheric convection over tropical oceans is strongly dependent on the two−fluid (atmosphere−ocean) interaction, a signature of the several atmospheric scales is expected to be found in oceanic field variables.

In fact, observations show that the horizontal structure of the Western Pacific warm pool is highly variable. Soloviev and Lukas (1997) analyzed ship measurements of the sea surface temperature (SST) and found sharp frontal interfaces of width 1−100m and separation 0.2−60km, several of them associated with precipitation−produced freshwater lenses. Due to the influence of the wind, most of the interfaces were anisotropic. Similar findings were obtained by Hagan et al. (1997) from aircraft measurements who established that horizontal temperature differences as large as 1oC may occur in less than 10km, in association with clouds and precipitation (cloud shadows and freshwater anomalies).

Several studies show that inhomogeneous surface forcing can modify atmospheric circulations, driving convection. Pielke et al. (1991) investigated how convection can be forced via sea−breeze circulations. Dalu et al. (1991) presented an evaluation of mesoscale disturbances driven by boundary−layer thermal inhomogeneities. They found that stronger mesoscale cells form when the wavelength of the forcing approaches the local Rossby radius; small−scale forcing producing mesoscale cells that interfere destructively to each other. Dalu et al. (1996) revisited this issue, in background wind conditions. Chen and Avissar (1994) showed that even with moderate background winds, land−surface wetness heterogeneities can produce significant changes on the mesoscale heat fluxes. Lynn et al. (1995) found that landscape discontinuities of various types can modify the atmospheric temperature, moisture content and moist static energy and concluded that the corresponding mesoscale processes have to be parameterized in general circulation models. Gopalakrishnan et al. (2000) tested various terrain wavelengths and verified that at scales as small as 5 km or less, roughness forcing has little impact. On the other hand, the authors showed that topographic features of very little vertical extent can change the boundary−layer statistics, if their horizontal scale is larger. Souza et al. (2000) also investigated convective circulations induce by land−surface contrasts.

Most of the previous work, however, focused on land−surface inhomogeneities, while the existence of a non−uniform SST and its possible impacts to the mesoscale structure of the atmospheric flow over oceans were often overlooked. Addressed in this paper is the hypothesis that inhomogeneous SSTs can modify atmospheric circulations not only on large scales, as well−known in climate studies, but also on the mesoescale, therefore influencing the organization of convection over tropical oceans. From this viewpoint, the highly variable horizontal thermohaline structure of the warm pool suggests a two−way coupling with the atmospheric variability. Significant horizontal gradients in skin−SST can be induced or dissipate on relatively short time scales by horizontal variations in the atmospheric fields, but in turn may generate cloud−scale and mesoscale circulations. Thus, it is necessary to determine to what extent SST inhomogeneities affect the collective properties of convective systems.

The present paper uses cloud−resolving simulations forced by prescribed, non−uniform SSTs to investigate the coupling of the atmosphere and the ocean on small timescales. The focus is on the influence of inhomogeneous SST in the organization of tropical convection. Section 2 describes the simulated case study briefly. In Section 3, the characteristics of the numerical model are presented. Results from three cloud−resolving simulations and a general discussion are presented in Section 4. Concluding remarks are summarized in Section 5.

2. CASE STUDY

During TOGA−COARE, an intensive observing period (IOP) took place from November 1992 through February 1993, in which enhanced meteorological and oceanographic monitoring was carried out. In order to achieve its goals, the COARE−IOP comprised an elaborate assemblage of observations from a variety of platforms in the ocean and the atmosphere (Webster and Lukas 1992). Figure 1 depicts the COARE sounding network, comprising a large−scale array

* *Corresponding author address*: Dr. Alexandre Costa. Universidade Estadual do Ceará, Departamento de Física e Química. Av. Paranjana, 1700. Campus do Itaperi. Fortaleza−CE, 60740−000. Brazil. E−mail: acosta@uece.br

(LSA), an outer sounding array (OSA) and the intensive flux array (IFA). The set of nested arrays was designed to provide a bridge from the large scales down to the IFA scale (Lukas et al., 1995). A significant part of the effort carried out during the COARE IOP was concentrated in the IFA area, including sounding sites, radar sites, research vessels, etc.

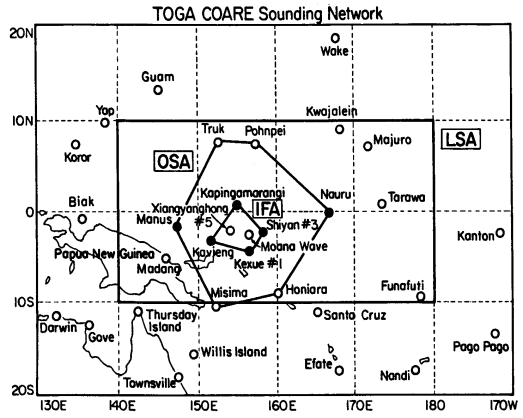

Figure 1 − The TOGA COARE sounding network (from Lin and Johnson, 1996a). Depicted are the large−scale array, the outer sounding array (OSA) and the intensive flux array (IFA). Observation sites are indicated.

According to Ding and Sumi (1995), atmospheric conditions during the TOGA−COARE IOP were similar to those of a developing warm episode over the eastern Pacific, including the frequent occurrence of westerlies in the lower troposphere, accompanied by upper−tropospheric easterlies. Lukas et al. (1995), however, pointed out that the TOGA−COARE IOP took place after an unusual evolution of the 1991/1992 warm event. Although the Southern Oscillation Index relaxed to zero prior to the experiment, the warm event intensified once again.

The COARE IOP was characterized by the occurrence of westerly wind bursts (WWBs). Sea−level pressure changes were associated with the strong westerly wind activity and corresponded to the re−intensification of the warm episode (Lukas et al., 1995). In fact, three prominent WWBs occurred over the COARE IFA during the IOP. Analyses of the flow over the IFA by Lin and Johnson (1996) contributed important findings for the understanding of the ISO structure over the WPWP.

The case simulated in this paper is the evolution of the cloud systems between 19 and 26 December 1992 during a WWB event (Case 2 of the GCSS Working Group 4, Moncrieff et al., 1997). The large−scale forcing for that period was constructed from the analyzed TOGA−COARE data (Lin and Johnson, 1996), obtained from soundings over the COARE intensive flux array (IFA). Figure 2 shows the evolution of the zonal wind (a), the vertical velocity in pressure coordinates (b), and the large−scale advective tendencies of temperature (c) and moisture (d), for that period.

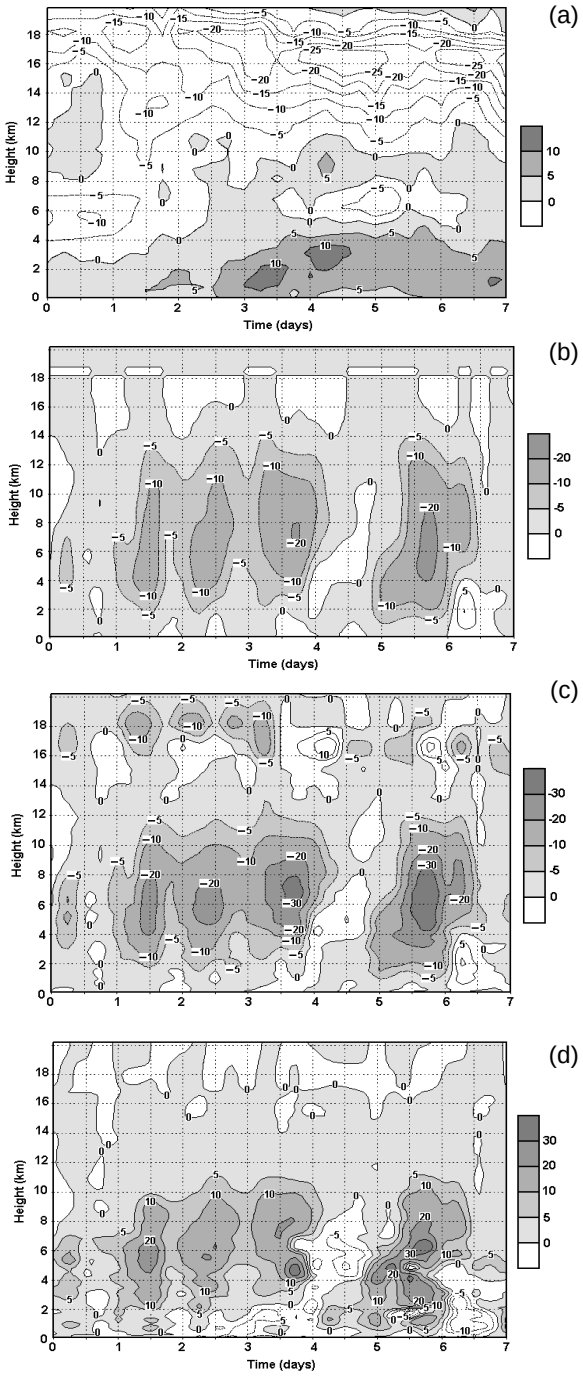

Figure 2 − (a) Observed zonal wind, in m.s−1; (b) omega, in mb.h−1; (c) temperature advection, in K.day−1; and (d) water vapor mixing ratio advection, multiplied by L/cp in K.day−1. Westerlies (panel a), ascending motion (b), cooling (c) and moistening (d) are in gray−scale. All fields are averages over COARE IFA between 19 and 26 December 1992.

As can be seen in Figure 2a, near−surface westerlies peak on 22 December. Large−scale rising motion prevails during most of the 7−day period, with the exception of 23 and 25 December. Peaks of large−scale advective cooling and moistening occurred on 20, 21, 22, and 24 December. As a result, significant convective activity occurred during most of the period, with the exception of 23 and 25 December. Between 19 and 26 December 1992, the SSTs experienced a general cooling trend, due to the strong surface fluxes associated with the WWB. The evolution of the average SST over the IFA is depicted in Figure 3.

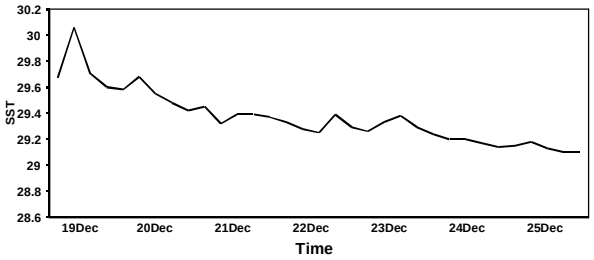

Figure 3 − Observed COARE IFA average SST, in oC, between 19 and 26 December 1992

3. CLOUD−RESOLVING MODEL

The atmospheric model used for this study is the Regional Atmospheric Modeling System (RAMS), developed at Colorado State University. As discussed by Pielke et al. (1992), RAMS has multiple options of numerical schemes and parameterizations and can be used in a wide spectrum of applications. RAMS have been successfully used in simulating both mid−latitude and tropical convection (e.g., Alexander and Cotton, 1998; Ziegler et al., 1997; Olsson and Cotton, 1997; Nair et al., 1997; etc.). In particular, as a cloud−resolving model, RAMS was used to investigate the sensitivity of tropical convective cloud systems to increased/decreased SSTs (Costa et al. 2001a) and coupled to an oceanic model to assess ocean−atmosphere feedbacks at small scales (Costa et al. 2001b).

3.1 *Numerical Schemes and Physical Parameterizations*

RAMS is a primitive equation numerical model solved on a Eulerian grid. The basic model equations are written in a non−hydrostatic, compressible form (e.g., Tripoli and Cotton, 1986). For the simulations performed here, a hybrid time−integration scheme was used, in which scalar fields were integrated using a forward−in−time scheme, and momentum fields were integrated using a centered−in−time (leapfrog) scheme. Second−order space differencing was used to represent advection.

The one−moment bulk microphysics includes seven categories of hydrometeors: cloud water, rainwater, pristine ice, snow, aggregates, graupel and hail or frozen raindrops (Walko et al., 1995). Ususally the hydrometeor concentration or size has to be prescribed by the user; the other being calculated from the model−predicted mixing ratio. The exception is the pristine ice category, for which a two−moment scheme that prognoses mixing ratio and concentration and diagnoses the ice crystal size. A summary of the microphysical settings used in our simulations is presented in Table 1.

Category	*Concentration scheme*	*Specified concentration*	*Specified mean diameter*	*Specfied width parameter*
Cloud water	Specified concentration	100 cm^{-3}	–	2
Rainwater	Specified mean diameter	–	1 mm	2
Pristine ice	Prognostic concentration	–	–	2
Snow	Specified mean diameter	–	1 mm	2
Aggregates	Specified mean diameter	–	1 mm	2
Graupel	Specified mean diameter	–	1 mm	2
Hail	Specified mean diameter	–	3 mm	2

Table 1 − Microphysical settings. For a given hydrometeor category, the number concentration can be user−specified, predicted, or diagnosed from the predicted mixing ratio and a user−specified mean diameter. A width parameter for the distribution−function is also specified (Walko et al., 1995).

A two−stream radiative scheme, coupled to the microphysics, and comprising three bands of short−wave and five bands of long−wave radiation (Harrington, 1997; Olsson et al., 1998) is used. Longitudinal variations of the incoming short−wave radiation are not considered. In order to save computer time, the tendencies to the thermodynamic equation due to radiative processes were updated every 10 minutes in our simulations.

The surface parameterization is the one by Louis et al. (1981), in which the fluxes are computed as a function of the roughness length, the Richardson number, the wind speed, and the differences of temperature and moisture between the air and the surface. A simple deformation−K closure (Smagorinsky, 1963), in which the influences of the Richardson number (Lilly, 1962) and the Brunt−Vaisala frequency (Hill, 1974) are considered, was used to represent sub−grid scale turbulence.

3.2 *Experimental Setup*

The model set−up followed much of the recommendations for the Case 2 of the GEWEX cloud systems study (GCSS) Working Group #4 (Moncrieff et al., 1997) and is similar to the model configuration used by Costa et al. (2001a, 2001b). RAMS was used in a two−dimensional mode, with a zonally−oriented

horizontal domain containing 512 model points, with a grid spacing of 1km along with a vertical grid of 50 points with variable resolution (100m to 500m grid spacing) and a 20.5 km depth. A timestep of 10s and periodic lateral boundary conditions were used.

The observed fields described in the previous section were ingested according to Grabowski et al. (1996). The initial wind, temperature and moisture profiles are horizontally homogeneous and correspond to the average IFA sounding on 19 December 1992. A nudging scheme was used to drive the model winds to the observations and forcing terms representing large−scale horizontal and vertical advection of heat and moisture over the IFA were added to the thermodynamic and water equations.

A random perturbation with an amplitude of 1K was imposed to the homogeneous, initial potential temperature profile, at the three lowest model levels, in order to trigger convection.

4. RESULTS

Sensitivity experiments were performed in which the mean SST was the same as the observed (Figure 3), but with superimposed sine function SST perturbations with a one−degree amplitude. Three different perturbations were tested, corresponding to "large" (256km, LARGE simulation), "medium−sized" (64km, MEDIUM simulation) and "small" (16km, SMALL simulation) wavelengths.

Most of the collective characteristics of the modeled convective systems were determined by the imposed large−scale forcing, as in Costa et al. (2001a). In addition, since the input of heat and moisture from the surface in LARGE, MEDIUM and SMALL were similar, the differences in the domain−averaged temperature and moisture fields were small. This is no surprise, since a sinusoidal perturbation integrates to zero for an integer number of wavelengths.

The vertical structure of the 6−day (20 to 26 December) mean of the domain−averaged cloud fields (various species of condensate, cloud fractional area, total cloud mass flux) was also very similar, and no significant sensitivity was detected.

Table 2 indicates the total, convective and stratiform precipitation in LARGE, MEDIUM and SMALL, as well as their respective rainy, convective and stratiform fractional areas (given by the number of model columns that exhibit rain, convective rain and stratiforme rain, respectively, divided by the total number of model columns, i.e., 512). The relative contributions of convective and stratiform columns to the precipitation were influenced by the horizontal dimension of the SST inhomogeneities, although the differences were only slightly larger than the variability found in the ensemble of multiple realizations of the CONTROL simulation in Costa et al. (2001a). In particular, LARGE exhibited more stratiform precipitation, while MEDIUM shows more convective rainfall.

Despite the similarities in most of the global characteristics of the cloud systems (constrained by the imposed large−scale forcing), including the total rainfall, there were noticeable differences in LARGE, MEDIUM and SMALL, related to the organization of the precipitation on the mesoscale in both time and space that can explain most of the differences reported in Table 2.

Variable	*LARGE*	*MEDIUM*	*SMALL*
Convective precipitation (mm/day)	14.5	15.1	15.0
Stratiform precipitation (mm/day)	6.3	5.5	6.0
Total precipitation (mm/day)	20.8	20.6	21.0
Convective fractional area (non−dim)	0.277	0.277	0.300
Stratiform fractional area (non−dim)	0.430	0.445	0.426
Total rainy fraction area (non−dim)	0.707	0.722	0.726

Table 2 − 6−day averages of the convective and stratiform precipitation, and fractional area covered by convective and stratiform rainfall in LARGE, MEDIUM and SMALL simulations between 20 and 26 December 1992.

Figures 4−6 represent Hovmöller diagrams of the surface precipitation rate for the three simulations with inhomogeneous SSTs. The panel corresponding to MEDIUM (Figure 5) has, in general, more small−scale structure, while in Figure 4, which shows the precipitation evolution in LARGE, coarse modes of the precipitation organization dominate. Apparently, SMALL does not show as many small−scale features as MEDIUM (Figure 6).

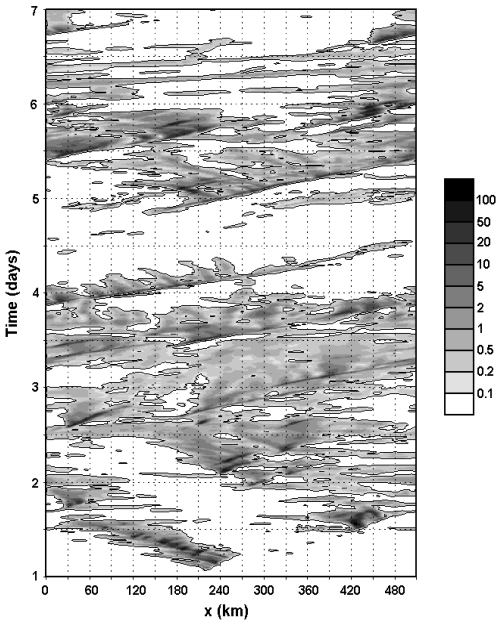

Figure 4 − Hovmöller diagrams of surface precipitation, LARGE, simulation. Gray levels represent different precipitation rates. The contour line represents 0.1 mm/h.

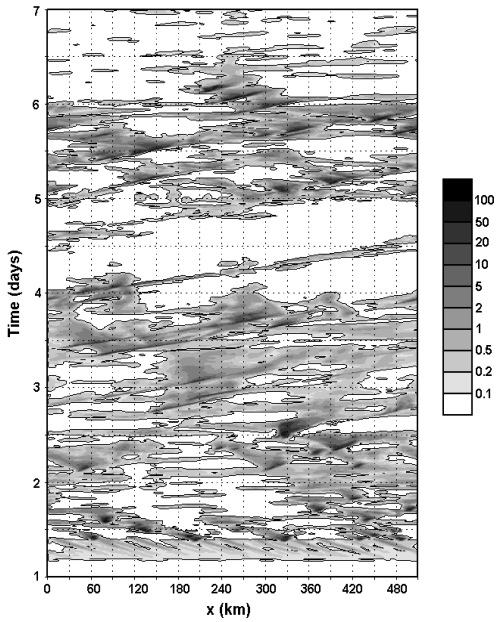

Figure 5 − Same as Figure 4, except for MEDIUM simulation

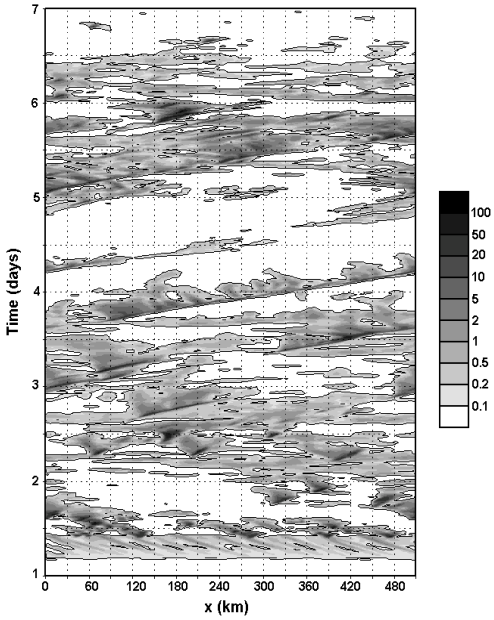

Figure 6 − Same as Figure 4, except for SMALL simulation

All diagrams show two dominant modes of convection organization: one is the "convective mode", corresponding to individual convective cells propagating eastward (In Figures 4−6, it appears as dark gray streaks with horizontal dimension on the order of a few kilometers); the other is the "mesoscale mode", corresponding to westward−propagating collectives of convective disturbances, which have stratiform precipitation from anvil clouds as their footprint (its signature in Figures 4−6 corresponds to light gray bands, tens to hundreds of kilometers wide, in which the convective cells are embedded). As suggested by Figures 4−6, the mesoscale mode is slightly inhibited in MEDIUM as compared to LARGE and SMALL. In particular, the systems formed after 3.5 and before 4.5 days of simulation (23 to 24 December) show more westward−moving stratiform precipitation in LARGE and SMALL and a greater occurrence of convective cells in MEDIUM. This is the period in which the large−scale forcing is weaker (Figure 2) enabling mesoscale circulations to show their signature more clearly.

Such differences become more evident in the spectral analysis of precipitation patterns. Let the two−dimensional Fourier transform of the surface precipitation field:

$$\hat{P}(\kappa,\omega)=\alpha\iint P(x,t)\mathrm{e}^{i(\kappa x-\omega t)}dxdt \qquad (1)$$

or

$$\hat{P}(\kappa,\omega)=\alpha\iint P(x,t)\mathrm{e}^{2\pi i(x/\lambda-t/T)}dxdt \quad , \qquad (2)$$

where P is the precipitation as a function of space and time, k is the wavenumber, l is the wavelength, w is the frequency, T is the period and a is an arbitrary constant, set to 1.0×10^{-4}(mm/day)$^{-1}$m^{-1}s^{-1}, resulting in a non−dimensional $\hat{P}$.

Averaging over the spatial scales, and looking at individual timescales, MEDIUM has the most prominent activity on the shorter timescale. The existence of more convective action in short timescales in MEDIUM is illustrated in Figure 7, which depicts $\hat{P}$ averaged over spatial scales up to 512km, for the time interval between 30 minutes and 2 hours. Between 10−12h, convection in MEDIUM is reduced; while SMALL and LARGE have comparable activities (Figure 8). Finally, LARGE has most activity on timescales larger than 12h (Figure 9). The conclusion is that SST perturbations with large wavelengths favored the organization of convection on the mesoscale and the development of stratiform precipitation. Surprisingly, the medium−sized SST disturbances generated more small−scale precipitation patterns and more convective precipitation than their small counterparts. Although the present system is obviously highly non−linear, this behavior can be compared to the one of a simple harmonic oscillator forced by an external agent. The external forcing produces little response if its frequency is much larger or much smaller than the natural frequency of the oscillator, but if the two frequencies are similar, resonance emerges. In addition, the effect in the atmosphere at the spatial scale of the SSTs in SMALL might be also homogenized significantly due to horizontal turbulence and horizontal advection as concluded in an analytic study of horizontal scales of

surface heating and their mesoscale response by Dalu et al. (1996).

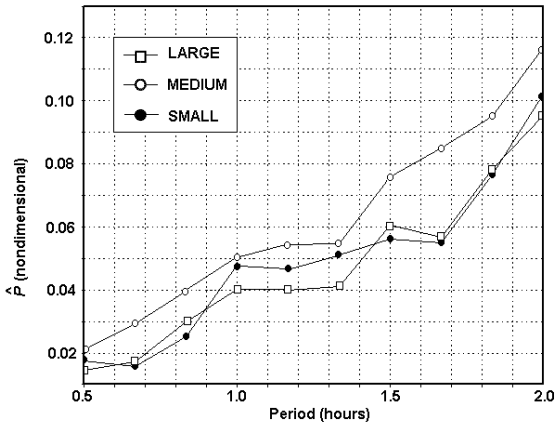

Figure 7 − Two−dimensional Fourier transformation of the surface precipitation, averaged over the spatial scales for timescales of less than 2h, in LARGE, MEDIUM and SMALL.

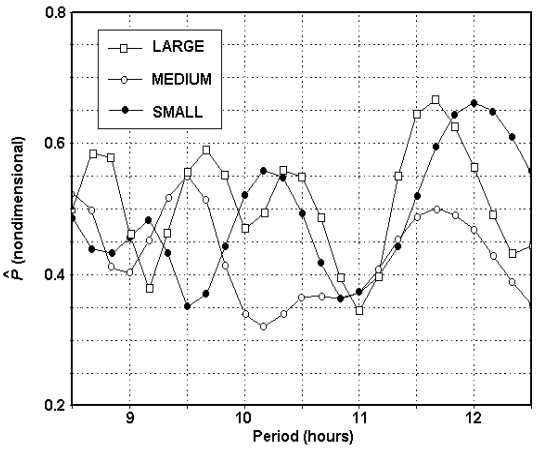

Figure 8 − Same as Figure 7, except for timescales between 8.5 and 12.5 hours.

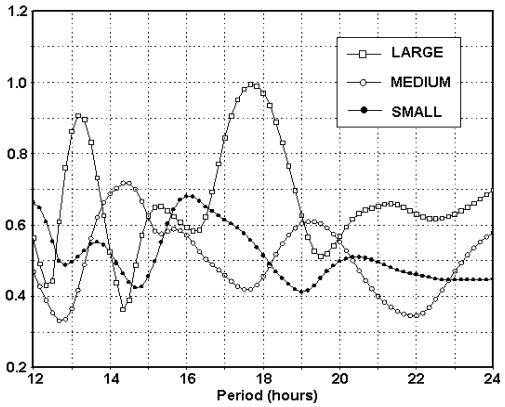

Figure 9 − Same as Figure 6, except for timescales between 12 and 24 hours.

5. CONCLUDING REMARKS

A significant variability was observed by several authors in the SST field over the Western Pacific warm pool, with sharp changes occurring on scales of the order of tens of kilometers or less (e.g., Hagan et al. 1997, Soloviev and Lukas 1997, Wijesekera et al., 1999). In order to investigate the influence of SST inhomogeneities of different wavelengths in the organization of atmospheric convection, idealized simulations were performed, in which sinusoidal perturbations were superimposed to the observed average SST.

Despite the similarities among most of the results from the simulations of inhomogeneous SST, different space−time organizational patterns were observed. Because convection is a non−linear process, the dominant atmospheric circulations (and precipitation patterns associated with them) can develop on a scale other than the one being forced. Large−scale SST perturbations induced circulations at coarse spatial and time scales, while medium−scale inhomogeneities tended to produce convective activity on smaller scales. Small−scale perturbations, however, did not favor convection at similar scales. The simulation in which the SST was varied using short wavelengths actually exhibited circulations in larges scales (on the order of several tens of kilometers).

A more detailed analysis of precipitation patterns via a Fourier analysis suggested that SST disturbances of medium−sized wavelengths favor the "convective mode" of organization and convective precipitation, while both large and small wavelengths favored a "mesoscale mode" and stratiform precipitation. Because a pattern with fluctuations on extremely small scales is virtually indistinguishable from another with no departures from the mean at all, one expects the existence of a point between, for which the influence of intermediate scales is maximized. The present results suggest that, for deep convection, such a point corresponds to a scale somewhat larger than the one of an individual cumulonimbus cloud. If the system is forced at a wavelength much greater or much smaller than its "natural wavelength", it shows little response. If the spatial scale of the surface forcing is optimum, i.e., corresponds to an average spacing between convective updrafts, the system's response is augmented. A simple analog is the harmonic oscillator forced at large or small frequencies versus frequencies close to its natural mode of oscillation. In the first two cases there is little response from the oscillator, while at the later case there is resonance.

Those conclusions agree with results from previous work, which show that there is an optimal wavelength for organizing mesoscale circulations, as proposed by Dalu et al. (1991) and that surface heterogeneities are not able to modify the characteristics of the mesoscale flow if their spatial scales are too small (Dalu et al. 1991, Gopalakrishnan

et al. 2000. Since the existence of background winds eventually masks some of the effects of a heterogeneous surface forcing (Chen and Avissar 1995, Dalu et al. 1996), idealized CRM simulations of quasi−equilibrium with and without background flow are suggested as future work.

ACKNOWLEDGEMENTS

This work was part of the author's Ph.D. studies at the Colorado State University, under Dr. William R. Cotton's supervision. Dr. Cotton is thankfully acknowledged, as well as Dr. Roger A. Pielke Sr., Dr. Robert L. Walko and Dr. Hongli Jiang, all from the CSU Atmospheric Department. Funding for this research was provided by the Conselho Nacional de Desenvolvimento Científico e Tecnológico (CNPq, Brazil) and the National Oceanic and Atmospheric Administration (NOAA, USA) under grant NA67RJ0152.

REFERENCES

Alexander, G. D. and W. R. Cotton, 1998: The use of cloud−resolving simulations of mesoscale convective systems to build a mesoscale parameterization scheme. *J. Atmos. Sci.*, **55**, 2137−2161.

Chen, F., and R. Avissar, 1994: The impact of land−surface wetness heterogeneity on mesoscale heat fluxes. *J. Appl. Meteor.*, **33**, 1323−1340.

Costa, A. A., W. R. Cotton, R. L. Walko, R. A. Pielke, Sr., and H. Jiang, 2001a: SST sensitivities in multi−day TOGA COARE simulations. *J. Atmos. Sci.*, **58**, 253−268.

Costa, A. A., W. R. Cotton, R. L. Walko, and R. A. Pielke, Sr., 2001b: Coupled ocean−cloud−resolving simulations of the air−sea interaction over the western Pacific. *J. Atmos. Sci.*, **58**, 3357−3375.

Dalu, G. A., R. A. Pielke, R. Avissar, G. Kallos, M. Baldi, and A. Guerrini, 1991: Linear impact of thermal inhomogeneities on mesoscale atmospheric flow with zero synoptic wind. *Annales Geophysicae*, **9**, 641−647.

Dalu, G. A., R. A. Pielke, M. Baldi, and X. Zeng, 1996: Heat and momentum fluxes induced by thermal inhomogeneities with and without large−scale flow. *J. Atmos. Sci.*, **53**, 3286−3302;

Ding, Y. H. and A. Sumi, 1995: Large−scale atmospheric circulation features during TOGA−COARE IOP. *J. Meteorol. Soc. Jpn.*, **73**, 339−351.

Grabowski, W. W., X. Wu, and M. W. Moncrieff, 1996: Cloud resolving modeling of tropical cloud systems during Phase III of GATE. Part I: Two−dimensional experiments. *J. Atmos. Sci.*, **53**, 3684−3709.

Gopalakrishnan, S. G., Roy, S. B., and R. Avissar, 2000: An evaluation of the scale at which topographical features affect the boundary layer using large eddy simulations. *J. Atmos. Sci.*, **57**, 334−351.

Hagan, D., D. Rogers, C. Friehe, R. Weller, and E. Walsh, 1997: Aircraft observations of sea surface temperature variability in the tropical Pacific. *J. Geophys. Res.*, **102**, 15733−15747.

Harrington, J. Y., 1997: The effects of radiative and microphysical processes on simulated warm and transition season Arctic stratus. Ph.D. dissertation, Atmospheric Science Paper No. 637, Colorado State University, Dept. of Atmospheric Science, 289 pp.

Hill, G. E., 1974: Factors controlling the size and spacing of cumulus clouds as revealed by numerical experiments. *J. Atmos. Sci.*, **31**, 646−673.

Lilly, D. K., 1962: On the numerical simulation of buoyant convection. *Tellus*, **2**, 148−172.

Lin, X., and R. H. Johnson, 1996: Heating, moistening and rainfall over the western pacific warm pool during TOGA COARE. *J. Atmos. Sci.*, **53**, 3367−3383.

Louis, J. F., M. Tiedtke, and J. F. Geleyn, 1981: A short history of the PBL parameterizations at ECMWF. Proceedings, Workshop on Planetary Boundary Parameterization, Reading, United Kingdom, ECMWF, 59−79.

Lukas, R., P. J. Webster, M. Li, and A. Leetmaa, 1995: The large−scale context for the TOGA Coupled Ocean−Atmosphere Response Experiment. *Meteor. Atmos. Phys.*, **56**, 3−16.

Lynn, B. H., D. Rind, and R. Avissar, 1995: The importance of mesoscale circulations generated by subgrid−scale landscape heterogeneities in General Circulation Models. *J. Climate*, **8**, 191−205.

Moncrieff, M. W., S. K. Krueger, D. Gregory, J.−L. Redelsperger, and W.−K. Tao, 1997: GEWEX cloud system study (GCSS) working group 4: precipitating convective cloud systems. *Bull. Amer. Meteor. Soc.* **78**, 831−845.

Nair, U. S., M. R. Hjelmfelt, and R. A. Pielke, Sr., 1997: Numerical simulation of the 9−10 June 1972 Black Hills storm using CSU−RAMS. *Mon. Wea. Rev.*, **125**, 1753−1766.

Olsson, P. Q. and W. R. Cotton, 1997: Balanced and unbalanced circulations in a primitive equation simulation of a midlatitude MCC. Part I: The numerical simulation. *J. Atmos. Sci.,* **54**, 457−478.

Olsson, P. Q., J. Y. Harrington, G. Feingold, W. R. Cotton, and S. M. Kreindenweis, 1998: Exploratory cloud−resolving simulations of boundary−layer Arctic stratus clouds. Part I: Warm season clouds. *Atmos. Res.*, **47−48**, 573−597.

Pielke, R. A., A. Song, P. J. Michaels, W. A. Lyons, R. W. Arritt, 1991: The predictability of sea−breeze generated thunderstorms. *Atmosfera*, **4**, 65−78.

Pielke, R. A., W. R. Cotton, R. L. Walko, C. J. Tremback, W. A. Lyons, L. D. Grasso, M. E. Nicholls, M. D. Moran, D. A. Wesley, T. J. Lee, and J. H. Copeland, 1992: A comprehensive meteorological modeling system − RAMS. *Meteorol. Atmos. Phys.*, **49**, 69−91.

Smagorinsky, J., 1963: General circulation experiments with the primitive equations. Part I: The basic experiment. *Mon. Wea. Rev.*, **91**, 99−164.

Soloviev, A., and R. Lukas, 1997: Sharp frontal interfaces in the near−surface layer of the ocean in

the western equatorial Pacific warm pool. *J. Phys. Oceanogr*., **27**, 999−1017.

Souza, E. P., N. O. Renno, and M. A. F. S. Dias, 2000: Convective circulations induced by surface heterogeneities. *J. Atmos. Sci.*, **57**, 2915−2922.

Tripoli, G. J. and W. R. Cotton, 1986: An intense, quasi−steady thunderstorm over mountainous terrain. Part IV: Three−dimensional numerical simulations. . *J. Atmos. Sci.*, **43**, 894−912.

Walko, R. L, W. R. Cotton, J. L. Harrington, M. P. Meyers, 1995: New RAMS cloud micro−physics parameterization. Part I: The single−moment scheme. *Atmos. Res.,* **38**, 29−62.

Webster, P.J. and Lukas, R. 1992: TOGA COARE − the coupled ocean atmosphere response experiment. *Bull. Amer. Meteor. Soc.*, **73** 1377−1416

Wijesekera, H. W., C. A. Paulson, and A. Huyer, 1999: The effect of rainfall on the surface layer during a westerly wind burst in the western equatorial Pacific. *J. Phys. Oceanogr.*, **29**, 612−632.

Ziegler, C. L., T. L. Lee, and R. A. Pielke, Sr., 1997: Convection initiation at the dryline: a modeling study. *Mon. Wea. Rev*., **125**, 1001−1026.